# RFTouchPads: Batteryless and Wireless Modular Touch Sensor Pads Based on RFID

**Meng-Ju Hsieh*** **Jr-Ling Guo*** **Chin-Yuan Lu*** **Han-Wei Hsieh***
**Rong-Hao Liang†** **Bing-Yu Chen§**
*§National Taiwan University †Eindhoven University of Technology
*{mjhsieh,jrling,chinyuanlu,hanweihsieh}@cmlab.csie.ntu.edu.tw †r.liang@tue.nl §robin@ntu.edu.tw

## ABSTRACT

This paper presents *RFTouchPads*, a system of batteryless and wireless modular hardware designs of two-dimensional (2D) touch sensor pads based on the ultra-high frequency (UHF) radio-frequency identification (RFID) technology. In this system, multiple RFID IC chips are connected to an antenna in parallel. Each chip connects only one of its endpoints to the antenna; hence, the module normally turns off when it gets insufficient energy to operate. When a finger touches the circuit trace attached to another endpoint of the chip, the finger functions as part of the antenna that turns the connected chip on, while the finger touch location is determined according to the chip's ID. Based on this principle, we propose two hardware designs, namely, *StickerPad* and *TilePad*. StickerPad is a flexible 3×3 touch-sensing pad suitable for applications on curved surfaces such as the human body. TilePad is a modular 3×3 touch-sensing pad that supports the modular area expansion by tiling and provides a more flexible deployment because its antenna is folded. Our implementation allows 2D touch inputs to be reliability detected 2 m away from a remote antenna of an RFID reader. The proposed batteryless, wireless, and modular hardware design enables fine-grained and less-constrained 2D touch inputs in various ubiquitous computing applications.

### Author Keywords

RFID; sensors; touch inputs; batteryless; wireless sensing; modular sensing.

## INTRODUCTION

Touch inputs are direct and intuitive. However, the deployment of touch sensors usually requires a signal processing unit (i.e., microcontroller) and a power supply. These extra hardware requirements limit the scalability and flexibility of the touch input deployment in ubiquitous computing applications [42].

Solutions that leverage computer vision or radio-frequency identification (RFID) can reduce their hardware requirements. Vision-based solutions [43, 45, 46] use one or more camera(s) to track touch events on a surface. However, such a tracking easily fails in the cases of occlusion. RFID-based solutions [18, 17, 49] use a wireless ultra-high frequency (UHF) reader to track touch events on UHF RFID tags, with the tracking being more resilient to the line-of-sight problems. Multiple RFID tags can be placed nearby each other to enable expressive gesture inputs such as swiping [18]. However, the size of the antenna required for the signal transmission limits the number of possible ways of the deployment of such a solution. For example, the tags cannot be deployed as a two-dimensional (2D) grid that is large and dense enough for capturing fine-grained, less-constrained touch inputs we normally perform on a touchscreen. Hence, the following question arises: *How can we enable fine-grained 2D touch inputs on RFID tags so that the scalability and flexibility of the solution remain uncompromized?*

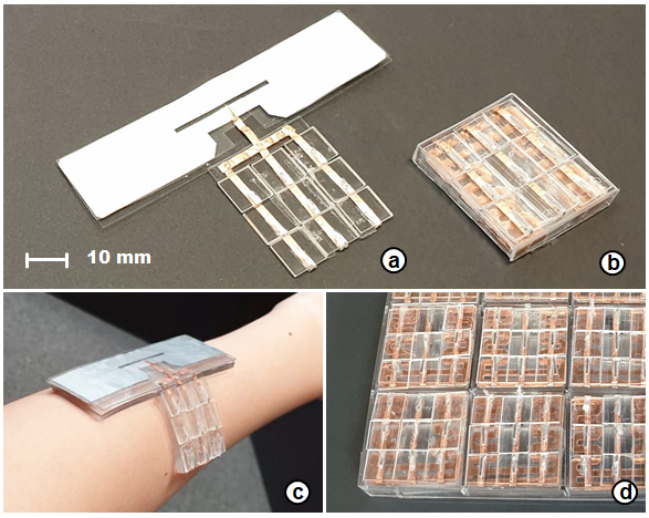


**Figure 1. RFTouchPads are batteryless and wireless modular touch sensor pads that support two-dimensional (2D) touch inputs based on ultra-high frequency (UHF) radio-frequency identification (RFID) tags: (a) StickerPad; (b) TilePad; (c) on-body StickerPad; (d) a grid of TilePads.**

In this paper, we present *RFTouchPads* (Figure 1), a system of batteryless and wireless modular hardware designs of 2D touch sensor pads based on the UHF RFID technology. This research takes an empirical approach to investigate possible solutions to the above-formulated question. First, we connected a single radio-frequency (RF) antenna to multiple touch-sensing identification (ID) modules in parallel to enable fine-grained 2D touch inputs (Figure 2). Similar to PaperID [17], each touch-sensing ID module connects only one of its endpoints to



*UIST '19,* October 20–23, 2019, New Orleans, Louisiana, USA



ISBN 978-1-4503-6708-0/20/04…$15.00

DOI: https://doi.org/10.1145/3313831.XXXXXXX

the antenna. This half-antenna design acts as an ungrounded monopole antenna that gets insufficient energy to operate, making the tag to be normally off and invisible to the reader. When a finger touches the circuit trace attached to an endpoint of a chip, the finger connects the userâĂŹs body that functions as part of the antenna structure, which improves the received signal power and turns the connected tag on. The presence of the tag identifies the finger touch event.

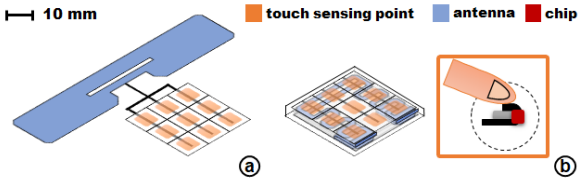


**Figure 2. Hardware overview: (a) StickerPad and (b) TilePad.**

We propose two module designs, *StickerPad* (Figure 1a) and *TilePad* (Figure 1b), based on the aforementioned touch-sensing principle to address the flexibility and scalability issues. StickerPad is a touchpad that provides 3 (Width; W)×3 (Height; H) $cm^2$ sensing area on a UHF tag, which is only 1.3-mm thick and flexible. The thin and flexible form of the StickerPad allows its applications to curved surfaces, or a human body with proper isolation (Figure 1c). TilePad is a tile with dimensions of 3.1 (W)×3.1 (H)×0.54 (Thickness; T) $cm^3$, which also provides 3×3 touch-sensing. The antenna of each module is redesigned to be folded to the back of the touchpad and still keeping a reasonable performance for supporting wireless touch-sensing. The TilePad design allows for a straightforward area expansion by tiling it as a grid (Figure 1d) that can support less-constrained 2D touch inputs. Such a small touch-sensing module enables a flexible deployment without being constrained by the tag antennas.

The implementations of our proposed designs were evaluated through a series of formal measurements. The results demonstrated that the proposed system can reliably detect 2D touch inputs remotely from a reader from a usable and applicable sensing distance. Furthermore, we present three applications: 1) on-body control using a StickerPad, 2) prototyping interaction devices using a grid of TilePads, and 3) adding interactivity to a piece of printed paper using TilePads to demonstrate the possible uses of these modules and how they can benefit the human-computer interaction (HCI).

The main contribution of this study is the designs of modular touch sensors based on modified UHF RFID tags that are batteryless, wireless, and easy to maintain. The modular design enables fine-grained and less-constrained touch inputs and meets the flexibility and scalability requirements of the practical applications in ubiquitous computing.

The rest of this paper is organized as follows. First, we present the proposed design principles and analyze the StickerPad and TilePad designs by evaluating their proof-of-concept implementations. Then, we present the three above-mentioned applications of the proposed designs. Finally, we discuss the limitations, design implications, and related work, as well as draw a conclusion.

## DESIGN PRINCIPLES

### Sensing Finger Touches Using a UHF RFID Tag

A conventional UHF RFID tag consists of a chip and an antenna, with the chip having two terminals connected to the antenna. As Li et al. demonstrated in their previous work [17], a conventional UHF RFID tag can be modified to be suitable for sensing finger touches. Figure 3a illustrates the design of a dipole UHF tag, which consists of a chip with its two terminals connected to an antenna to receive energy for signal transmission. This tag can be disabled by cutting at least one of the two terminal connection to the antenna (Figure 3b) because the energy received through one connection is not sufficient for signal transmission. When the human finger touches the terminal, it connects the human body to the tag. As such, the human body functions as a ground plane of the antenna that improves the energy harvesting by the wireless signal source, enabling the tag to transmit signals (Figure 3c). Such a state transition between the absence and presence of the ID can be recognized as a touch event.

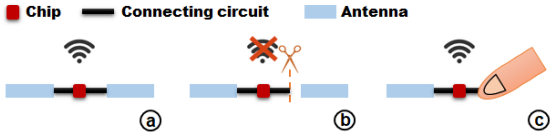


**Figure 3. Sensing finger touches using a UHF RFID tag: (a) a dipole UHF RFID tag; (b) one pole of the tag is cut to disable the tag; (c) the tag is enabled when a finger touches the open terminal.**

Although this mechanism was demonstrated to work reliably, the resolution of the touch sensing is limited by the antenna, which occupies most of the tag space. While using tags with smaller antennas could remedy such a limitation of the sensing resolution straightforwardly, this would compromise the sensing distance. Since the wireless sensing distance is the key factor for such an RFID-based technology to be deployed in ubiquitous computing applications, the major challenge is to increase the sensing resolution while preserving a usable and applicable sensing distance.

### Increasing the Touch-Sensing Resolution

Connecting multiple touch-sensing elements to a shared antenna as a multi-chip tag can be a feasible solution. While previous studies have shown the feasibility of a shared antenna for connecting multiple chips [2, 3, 4, 23], its application to tracking fine-grained 2D touch inputs has not been achieved yet.

Figure 4 illustrates our method for connecting multiple chips on a shared antenna. First, we detach the sensing element, which is a chip with a short circuit trace connected to its both terminals, from the tagâĂŹs antenna. Then, we bend the component and put a plastic sheet in between the two circuit traces for isolation. Then, we connect the elements in parallel, and finally, affix the parallelized elements to a shared antenna.

Such a multi-chip design can provide multiple touch-sensing points with a high density since the circuit bending can be achieved within a small radius. However, we should not expect these components to be connected in an infinite length

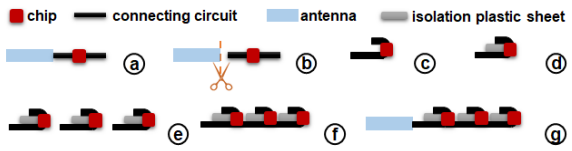


**Figure 4. Principles of making a multi-chip tag: (a) touch-sensing UHF RFID tag; (b) cutting a part of trace with the chip; (c) bending and (d) isolating the trace to make a touch-sensing point; (e) and (f) connecting multiple touch-sensing points in parallel; (g) attaching the touch-sensing points to the antenna.**

to achieve the size expansion because the energy harvested from the antenna is limited. Instead, we should limit the number of connected components to a usable value and consider expanding the sensing area through hardware modulization.

### Increasing the Touch-Sensing Area

Sensor tiles are modules that can support the expansion of the sensing area straightforwardly. To support the regular tiling operations, the employed sensor should be made as a regular $P_n$ polygon, where n can be 3, 4, or 6. Without loss of generality, we choose $n = 4$ for our design. The idea is to make square sensor modules that are laterally tileable, with the sensing elements being uniformly distributed on the surface of each module. Therefore, the key challenge is to reduce the antenna used in the touch-sensing area. Folding the antenna to the back of the sensing area allows us to make a three-dimensional (3D) multi-chip tag to achieve this goal.

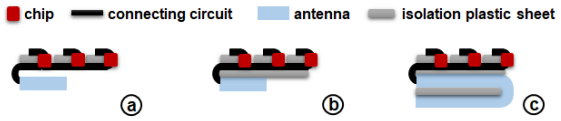


**Figure 5. Principle of making a three-dimensional (3D) multi-chip tag: (a) folding the antenna; (b) using a sheet to isolate two layers; (c) extending the length of the antenna.**

Figure 5 illustrates our method for producing a 3D multi-chip tag. First, we bend the antenna to the back of the sensing area, and then, put a plastic sheet in between the sensing layer and the antenna layer for isolation. Notably, with this design, we can further extend the length of the antenna layer by folding it back and forth, as demonstrated in Figure 5c. In this way, we may compensate for the sensing distance loss.

### Sensor Deployment for Everyday Surfaces

Figure 6 shows the plausible ways for the sensor deployment. The sensor pad can be directly affixed to the surface of a non-conductive material or object to achieve the touch sensing (Figure 6a), similar to the way how UHF RFID tags are used. However, when an RFTouchPad is attached to a human body, a proper isolation is required to maintain the separation between the sensor pad and the skin (Figure 6b). Without such an isolation, the sensing range of a UHF antenna would be significantly reduced due to the proximity of the human body [26]. Last but not least, the inductive sensor pad allows the touch to be detected through a thin layer (Figure 6c) of non-metallic materials such as paper that can hide the sensors or provide an additional affordance [6] for the user interaction. When a finger is in a close proximity to the terminal, it improves the signal power that can turn the tag on. The thickness of the covering sheet may affect the wireless sensing range of the sensor pad.

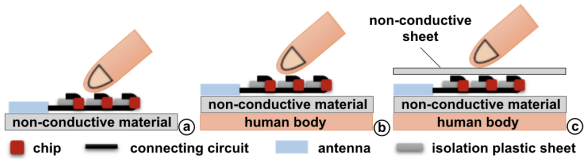


**Figure 6. Sensor deployment: (a) directly attaching the sensor pad to the surface of a non-conductive material; (b) attaching the sensor pad to a human body with a piece of a non-conductive material placed in between; (c) covering the sensor pad with a thin non-conductive sheet.**

### Summary

The proposed design provides a feasible way to achieve our goals by enabling fine-grained, less-constrained touch inputs using the UHF RFID tags. These touch sensor pads can be deployed on everyday surfaces to enable touch inputs. Nonetheless, several unknown design parameters still remain, including the number of the sensing elements in the multi-chip design, size and thickness of the 3D multi-chip sensor grid, and thickness of the covering and isolation layers. We clarify these factors by analyzing several designs of RFTouchPads.

## DESIGNING STICKERPADS

We investigated the feasibility of implementing multiple-touch points on a single tag for enabling fine-grained 2D touch inputs. Three types of UHF RFID tags, namely, AZ-9654 [93 (W)×19 (L) $mm^2$], AZ-9662 [70 (W)×17 (L) $mm^2$], and E41-C [95 (W)×8 (L) $mm^2$], were selected as they have similar physical dimensions and a sensing distance of 6 m but different antenna designs (i.e., different ratios between the meander-lines and the radiators). Ten tags of each of the three types were selected and tested. For each tag, we removed its chip and attached the Monza 4 chip [0.7 (W)×0.7 (L) $mm^2$] instead. Figure 7 illustrates the implementation of the single-point touch sensor design according to our previously introduced sensing principle.

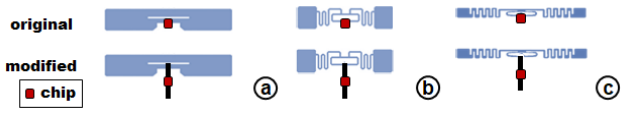


**Figure 7. Illustration of the proposed UHF touch sensor implementation: (a) AZ-9654; (b) AZ-9662; (c) E41-C.**

### One-dimensional StickerPads

Figure 8 illustrates our implementation of one-dimensional (1D) StickerPads. Low-ohmic 3M 1181 copper foil shielding tapes were used for connecting multiple Monza 4 chips in parallel. We set the pitch between each tag to 1 cm, which is small enough and allow us to test each touch point using a fingertip. The small pitch also serves its purpose of detecting fine-grained touch inputs. 1-mm (T) plastic sheets were used between the bent circuit traces for insulation. We conducted a series of formal measurements to understand the performance of our implementation.

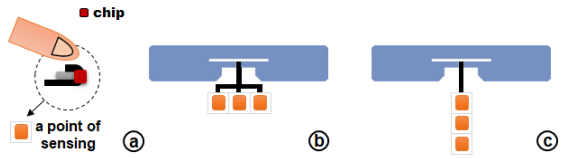


**Figure 8. 1D StickerPads: (a) illustration of a touch-sensing point; (b) 3×1 horizontal connection; (c) 1×3 vertical connection.**

### *Evaluation*

*Apparatus.* Figure 9a illustrates the experimental apparatus installed in an empty space with dimensions of 3 (W)×5 (L)×3 (H) $m^3$. During the measurement, each tag was mounted on the center of a wooden table with a height of 32 cm arranged in the center of the room, serving as the measurement platform. An ANT925SMA circular polarized antenna was fixed under table 20 cm away from the measurement point. The signal band was configured to be between 902 MHz and 928 MHz, while the signal amplitude was set to 32.5 dB. The antenna was wire-connected to an Impinj Speedway Revolution R420 UHF RFID reader, which was placed under the antenna.

*Procedures.* A tag with two touch-sensing points, which were in either the vertical or horizontal connection, was placed on the central surface of the table. Every touch-sensing point was tested three times to ensure that they can serve as touch sensors connected into a chain. If a test point failed in detecting a touch in any of the trials, the round was terminated. Otherwise, another touch-sensing point was added to the connection until not every touch event could be detected at all the touch points, the length of the sensor chain in the previously successful round was recorded. A total of 60 rounds were conducted (3 antennas×10 tags×2 directions×1 trial).

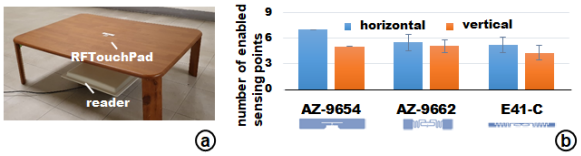


**Figure 9. (a) Experimental apparatus. (b) Connection lengths of the fully-working 1D StickerPads. The AZ-9654 implementation is the most stable compared to the others.**

*Results.* Figure 9b demonstrates that the AZ-9654 tags were the most stable version of the proposed design implementation. In particular, they detected every touch in M = 7.0 (SD = 0) point-length horizontal connection and M = 5.0 (SD = 0) point-length vertical connection. The AZ-9662 [horizontal: M = 5.5 (SD = 0.97); vertical: M = 5.1 (SD = 0.74)] and E41-C [horizontal: M = 5.2 (SD = 0.92); vertical: M = 4.3 (SD = 0.82)] tags were less stable and supported shorter lengths in general. Therefore, we chose the antenna of the AZ-9654 tags for further studies due to its stable touch sensing.

## Two-Dimensional StickerPads

Based on the results of the preliminary experiment described in the previous section, we used the AZ-9654 tags to implement 2D StickerPads. Each StickerPad consisted of a 2D grid of touch-sensing points with a 1-cm pitch, and the implementation was extended from the previously presented 1D StickerPads. Figure 10a illustrates an example implementation of a 3×3 touchpad. Based on the above-presented results, four sizes (2×2, 3×3, 4×4, and 5×5) were implemented. In addition, we conducted a series of formal measurements to understand the performance of our implementation.

### *Evaluation*

*Apparatus and Procedures.* The experimental apparatus was the same as for the above-presented study of the 1D StickerPads (Figure 9a). The procedures were also similar to those of the study of 1D pads. Different sizes of N×N 2D connections, where N≥2, were tested. N = 2 was tested first, and every touch point was tested three times to ensure that they can serve as touch sensors connected into a chain. Then, we increased the size of the StickerPad to N+1×N+1 until N = 5. If not every touch event could be detected at all touch points, the previously successful round of the size was recorded. A total of 2160 trials were performed [10 tags×(4+9+16+25) touch points×3 trials].

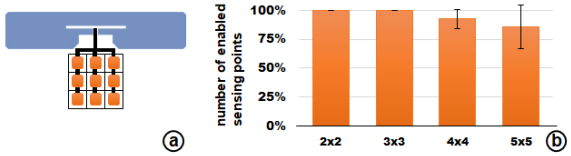


**Figure 10. (a) Example 3×3 StickerPad. (b) Number of enabled touch-sensing points in four sizes. The touch-sensing points are reliable on both 2×2 and 3×3 StickerPads.**

*Results.* Figure 10b shows the results. All 10 tags detected every touch on both 2×2 and 3×3 StickerPads. This result demonstrates that the AZ-9654 implementation can reliably support fine-grained 2D inputs on a StickerPad that consists of a 3×3 grid of 9 touch points. The accuracy of the 4×4 and 5×5 pads was 92.5% (444 out of 480 trials) and 85.7% (643 out of 750 trials), respectively. Among all, four 4×4 and three 5×5 pads reached an accuracy of 100%, demonstrating that chaining 16 or 25 sensing points to one antenna is practically feasible. The tags that failed shared the same design with the successful tags. Since the AZ-9654 antenna was proved to be stable in the first study, we argue that the 3×3 StickerPad, which was 100% accurate in all the 10 trials, is our current capability of a reliable fabrication.

## Implementation

Based on the results of the first two studies describe above, the StickerPad was implemented by attaching a 3×3 touchpad with a 1-cm pitch to the AZ-9654 antenna. A 0.3-mm (T) plastic sheet was added to the back of the antenna and touchpad as a physical support, which also allowed applying an adhesion without damaging the circuit traces. In our testing environment, this module reliably supported the touch sensing within a sensing distance of 4 m with a single-antenna UHF reader, when it was attached to the surface of a non-conductive material as illustrated in Figure 6a. The sensing area of four 3×3 StickerPads was tiled as a 2×2 grid, where the 36 touch-sensing points were placed inward, whereas the antennas were placed outward (Figure 11). Nonetheless, the large antenna still occupied a significant space and it could not be tiled further.

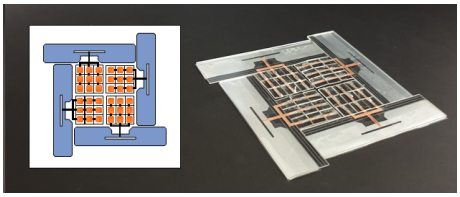

**Figure 11. Four 3×3 StickerPads providing 6×6 touch-sensing points in a 6×6 cm$^2$ sensing area.**

## DESIGNING TILEPADS

We further investigated the feasibility of implementing tileable StickerPads, called TilePads, to achieve a modular expansion of the touch-sensing area. The fundamental solution was to fold the antenna of a StickerPad behind its touchpad to make the size of the moduleâĂŹs footprint to be equal to the sensing area as shown in Figure 12. The antenna could be folded to the back of a touchpad, while the excessive length of the antenna could be folded into an origami structure. However, we found that such folding operations affected the touch-sensing performance since the implementation shown in Figure 12c could support no more than six out of nine touch points. Other possible designs illustrated in Figure 13 demonstrated even worse performance.

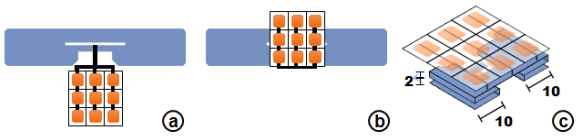


**Figure 12. Folding a StickerPad: (a) original StickerPad; (b) folding the antenna behind the touchpad; (c) folding the excessive length of the antenna into an origami structure.**

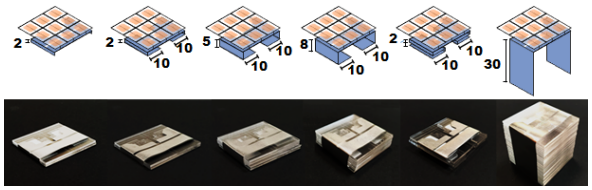


**Figure 13. Types of antenna folding that failed during our exploration.**

The AZ-9654 antenna was not designed for folding; hence, it required multi-step folding as illustrated in Figure 12. We hypothesized that the multiple folding operations were the main reason for the performance drop. Therefore, the goal of the antenna redesign was to enable one-step folding that could not be simpler.

### Designing One-Fold Antenna for TilePads

A one-fold antenna can be realized by reducing the size of the antenna to 3 (W)×3 (L) cm$^2$, which is the same size as a 1-cm-pitch 3×3 touchpad. To utilize such a limited space, we adopted three antenna designs, namely, *radiators* (Figure 14a), *meander-lines* (Figure 14b), and *meander-radiators* (Figure 14c), which have been proven to be effective in small RF antenna designs [28, 22]. To make the results comparable to the original AZ-9654 antenna, we designed the antenna to be symmetric as well. In addition, we shortened the connectors to maximize the size of the antenna (Figure 14d). We conducted a series of formal measurements to understand the performance of the proposed antenna designs.

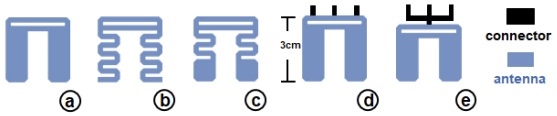


**Figure 14. One-fold antenna designs: (a) radiators; (b) meander-lines; (c) meander-radiators; (d) shortened connector; (e) original connector.**

#### *Evaluation*

*Apparatus and Procedures.* The experimental apparatus was the same as that in the study of 2D StickerPads. A total of 30 antennas were tested (3 types×10 antennas). All antennas were tested with the same 3×3 touchpad. For the touchpad attached to each of the antenna, every touch point was tested three times to ensure that they can serve as touch sensors. A total of 270 touches were recorded (3 types×10 antennas×9 touch points).

*Results.* Figure 15b shows that the one-fold meander-lines design reliably detected a mean number of M = 8.7 (SD = 0.47) out of 9 touches on the 3×3 touchpad, significantly outperforming the other two designs. All three one-fold designs activated a M = 7.35 (SD = 1.44) out of 9 touches, which also supports our hypothesis that the redesigned one-fold antennas can outperform the original AZ-9654 antenna. We used the meander-lines design (Figure 15d) for further investigation.

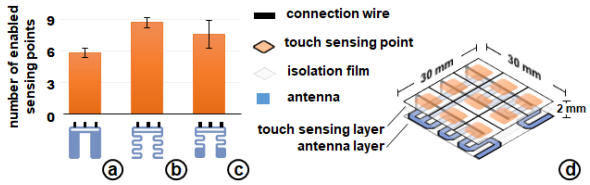


**Figure 15. Number of enabled touch-sensing points in one-fold antennas: (a) radiators; (b) meander-line; (c) meander-radiators. (d) Overview of the meander-line design.**

### Extending the Antenna to Achieve a Better Sensitivity

The one-fold *meander-lines* design did not fully enable the sensing of 3×3 touch inputs as not every touch was detected in the 10 samples of the test. We expected to minimize the likelihood of having such defects since the modules were made for tiling. Hence, we extended the length of the antenna to see if it can improve the sensitivity of touch sensing.

Figure 16 demonstrates the concept of the antenna extension. The length of the antenna can be extended arbitrarily. For instances, Figures 16a to 16d show three different ratios (33%, 67%, and 100%) of the extension. Moreover, the extension can be folded back and forth in multiple layers as demonstrated in the two-layer example shown in Figures 16e to 16g. The extension can be implemented using either meander-lines or radiators. We used a 1-mm (T) plastic sheet for the isolation between each layer. We conducted a series of formal measurements to understand the performance of these antenna designs.

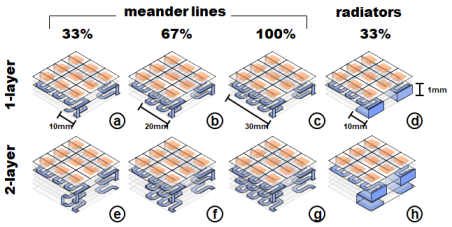


**Figure 16. Examples of extended antennas with various coverage ratios and layers of back-and-forth folding using meander-lines and radiators.**

### *Evaluation*

*Apparatus.* The experimental apparatus was the same as that in the study of one-fold antennas. Three different coverage ratios (33%, 67%, and 100%) in five numbers of layers of back-and-forth folding (1, 2, 3, 4, 5) were tested with two types of extensions (*meander-lines* and *radiators*). All antennas were tested using the same 3×3 touchpad.

*Procedures.* After the touchpad was attached to each of the antennas, we tested every connection to be $< 1\Omega$. Then, every touch point was tested in an order of 9×9 Latin Square, and every touch event lasted for 1 second. A total of 2700 touches were tested (3 ratios×5 layers×2 types×10 antennas×9 touch points).

*Results.* Figure 17 shows that the extension using *33% radiators* reliably detected every touch in 1, 2, and 3 layers of back-and-forth folding, outperforming the other designs and demonstrating an enhanced performance compared to the non-extended design. Nonetheless, in the cases of 4 and 5 layers of back-and-forth folding, the complexity of folding did affect the performance of the radiator-based extension. The 33% ratio extension, which covered only 1/3 of the touch-sensing area, outperformed the other two ratios (67% and 100%) in the extensions using *meander-lines* and *radiators*. This demonstrates why simply folding the AZ9654 antenna as shown in Figure 13 could not work. Among all, we used the *33%-radiators*-based extension for further investigation.

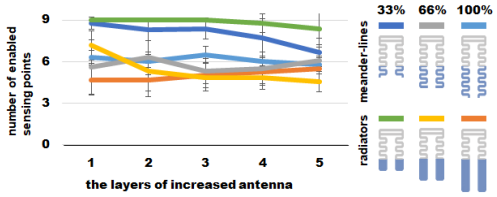


**Figure 17. Results of the touch-sensing performance with different antenna extensions. The *33%-radiators*-based extension reliably detected every touch in 1, 2, and 3 layers of back-and-forth folding.**

### Sensing Distance vs. Number of Extension Layers

We further investigated the sensing distance of the extended one-fold antenna regarding the number of back-and-forth folding layers.

*Apparatus.* Figure 18 illustrates the experimental apparatus, which was installed in the middle of an empty corridor with dimensions of 3 (H)×3 (W)×12 (Length; L) $m^3$. The antenna and reader, which had the same settings as the ones used in the testing of the StickerPad, were fixed on one plastic pillar. A touchpad was fixed to another plastic pillar at the corresponding location of the antenna. The location and direction of the touchpad were carefully aligned so that only the distance between the sensor and the antenna was changed. Based on the previous results, meander-line antennas with 1, 2, and 3 layers of the *33%-radiator*-based extension were tested. All antennas were tested with the same 3×3 touch pad.


**Figure 18. Experimental apparatus.**

*Procedures.* The experimental procedure was similar to that of the previous study of the antenna extension. The sensor was tested at five distances (1, 2, 3, 4, and 5 m away from the reader) in 3 iterations. A total of 4050 touches were recorded (3 layers×5 distances×10 antennas×3 iterations×9 touch points).

*Results.* Figure 19 shows that the extended antennas with 2 and 3 layers of back-and-forth folding reliably detected every touch at a distance of 2 m. The extended antenna with only 1 layer of folding worked at a distance of 1 m but failed at a distance of 2 m.

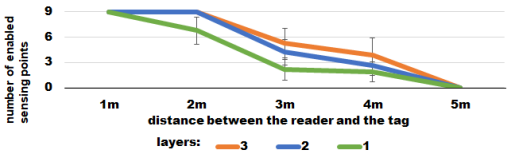


**Figure 19. Extended antennas with 2 and 3 layers of back-and-forth folding reliably detected every touch at a distance of 2 m.**

### Implementation

Figure 20a illustrates the TilePad design, which was concluded from the results of our previous studies. The 3×3 touchpad was attached to a meander-line antenna with the two-layer folded 33%-radiator-based extension. A 0.5-mm (T) isolation frame was added to the module to prevent the incidental contact of the nearby modules when tiling. The dimensions of the TilePad module were 3.1 (W)×3.1 (L)×0.54 (T) $cm^3$. The module supported the touch sensing within a sensing distance of 2 m for a single RFID antenna. Figure 20b illustrates a grid of 5×5 TilePads providing 15×15 touch points in a sensing area of 15.5 (W)×15.5 (L) $cm^2$. All touch points were tested to be functional in the same setting as that used in our previous experiments.

## SENSOR DEPLOYMENT

A touch sensor pad can be deployed on the body for on-body applications (Figure 6b). Furthermore, the user can deploy a non-conductive sheet on the top to provide visual cues or for embedded uses (Figure 6c). We conduct a preliminary investigation on how these alternative deployments could affect the sensing performance of the proposed touch pads and highlight feasible solutions.

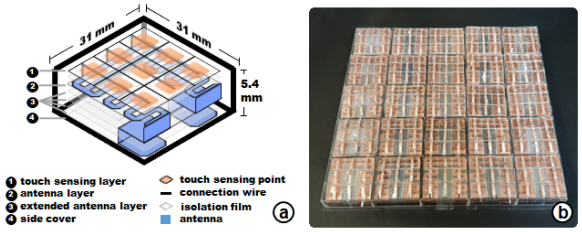


**Figure 20. (a) TilePad design; (b) 5×5 grid of TilePads providing 15×15 touch points in a sensing area of 15.5 (W) ×15.5 (L) cm$^2$.**

### Sensing Distance vs. Body Proximity Problem

The human body behaves as an inhomogeneous lossy antenna for the UHF signals; hence, it degrades the tagâĂŹs performance when being in a close proximity with it [26]. It has been verified that the separation of a tag antenna from the body surface larger than 1 cm suffices to reduce the detrimental body effects. At the same time, a 1-cm separation might be considered significant in on-body applications. Therefore, we investigated this issue through a two-round experiment with multiple users since the effects may vary across multiple users.

The experimental parameters were determined in the first round. A TilePad, a StickerPad, and flexible plastic sheets with a thickness of 1, 2, and 3 mm were tested using the apparatus illustrated in Figure 18. A female user (age = 24) was recruited to test the distance limitation of the TilePad and StickerPad with the plastic sheets, which were used as the isolation between the sensor pads and the skin. With her forearm being lifted toward the antenna, the user touched the isolated pad on her forearm that was placed 0.1 m away from the reader. If all 9 points were detected, the user moved 0.1 m backward and tried again; otherwise, we recorded the distance limitation. After several trials, the results demonstrated that the TilePad can work at a distance greater than 2 m with just 1-mm-thick isolation because its touch-sensing surface is already 5.4 mm away from its bottom. The StickerPad was found to be working at a sensing distance greater than 2 m with a 3-mm-thick isolation.

The parameters identified in the first round were used in the second round of testing. Ten participants (five males and five females) aged between 21 and 28 (M = 23.8, SD = 1.99) were recruited for testing the 1-mm-isolated TilePad and a 3-mm-isolated StickerPad. The participants had a BMI ranged between 16.2 and 24.8 (M = 20.47, SD = 2.57). The apparatus and procedures were the same as mentioned previously. The results demonstrated that, across all subjects, the TilePad worked at a mean distance of 2.17 m (SD = 0.13), whereas the StickerPad worked at a mean distance of 2.1 m (SD = 0.12). The low standard deviation for StickerPad suggests its stability of the touch sensing across the ten users.

Figure 21 illustrates our implementation of the on-body StickerPad, which provided a sensing distance of 2 m in our experiment setting. To retain the flexibility of the original StickerPad (Figure 21a), the 3-mm-thick isolation was implemented using a flexible plastic sheet (Figure 21b-c) or sponge sheet (Figure 21d) to meet the requirement of flexible deployment. Future work can also consider using waterproof polydimethylsiloxane (PDMS) for a tight integration between the sensor and the isolation sheet [15] to allow its washing.

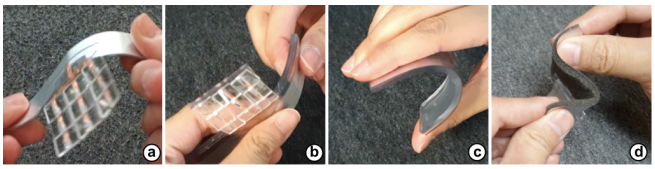


**Figure 21. (a) Original StickerPad. (b)(c) StickerPad with a 3mm-think flexible plastic sheet. (d) StickerPad with a 3mm-think sponge.**

### Sensing Distance vs. Covering Sheet Thickness

Without loss of generality, we tested the thickness of the non-conductive sheet using 70 g/m$^2$ paper with a thickness of 0.09 mm. A visual content could be printed on top of the sheet as the visual affordance for HCI. A TilePad, a StickerPad, and five pieces of 70 g/m$^2$ paper were tested using the apparatus illustrated in Figure 18, where the antenna was fixed to one plastic pillar, while a touchpad was fixed to another plastic pillar at the corresponding location of the antenna. The location and direction of the touchpad were carefully aligned so that only the distance between the sensor and the antenna could be changed. A user tested the pads using the same procedures as described for the body proximity testing. According to the results, when the paper amount increased from 1 to 5 pieces, the sensing distance of the TilePad gradually reduced from 1.5 m to 0.9 m, while the sensing distance of the StickerPad gradually reduced from 2.6 m to 1.5 m. Hence, we can conclude that the covering sheet should be as thin as possible to retain a high sensing distance.

## APPLICATIONS

Based on our implementation and experimental apparatus, we present several room-scale applications of the RFTouchPads.

### Controlling a Playlist with an On-Body StickerPad

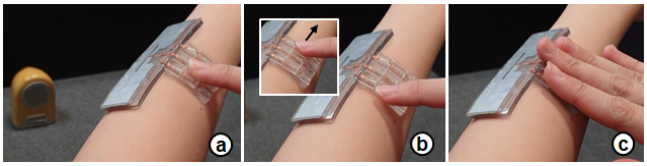


**Figure 22. On-body playlist controller. The user (a) plays a song with a long pressing, (b) switches to the next song by swiping right, and (c) covers the entire pad to pause the song.**

The StickerPad can be applied to the forearm as a sticker and used as an on-body music playlist controller. As shown in Figure 22, a user can play and pause a song at the top of the playlist by long pressing the touchpad using her fingertip, as well as switch to the next or previous song by swiping right or left, respectively. She can also pause the playlist by covering the entire touchpad, which is easier to perform without looking at the touchpad.

The StickerPad is reliable as it is normally turned off and only reacts to a physical touch. This batteryless and wireless controller is inexpensive and disposable; hence, it is suitable for being deployed at scale in applications such as interactive exhibitions. The antenna can be designed in an aesthetic manner so it could be fashionably worn similar to a tattoo sticker.

### Prototyping Touch Input Devices with a Grid of TilePads

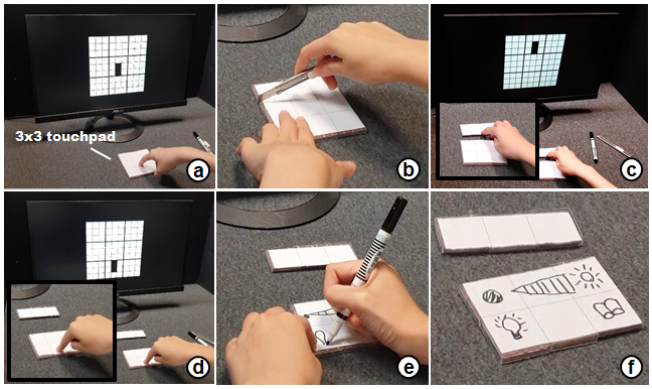


**Figure 23. Prototyping a kit of touch devices: (a) a grid of paper-covered 3×3 TilePads; (b) trimming the sensor to the desired size; (c) and (d) testing both parts of the touch sensor; (e) drawing widgets on the screen with a marker pen; (f) results.**

A grid of TilePads can be used as a kit of prototype input devices for HCI. Figure 23 illustrates a grid of 3×3 TilePads covered by a thin piece of paper, which allows scribbling and for the finger touch to be detected. To make a control panel, a user can cut a 2/3-portion of the grid with a knife and use a marker pen to draw the desired widgets on its surface.


**Figure 24. Operation binding: (a) touching both on-screen and hand-drawn widgets to start the binding; (b) moving hands to record the correspondence; (c) releasing the hands to commit the binding.**

Figure 24 demonstrates how to bind the control operations to the hand-drawn widgets. The user touches the on-screen virtual widget with one hand and hand-drawn widget with another hand. Then, the user moves his both hands at the same time to record the correspondence between the two widgets and releases the on-screen widget to commit the binding. Meanwhile, the server connected to the RFID reader updates its configuration. After several functions are bound, one can use this self-made control panel as an additional remote controller for a smart lighting in the room (Figure 25).

Figure 26 demonstrates that the remaining 1/3 of the sensor grid can still be used for prototyping other input devices. The user uses a 1×2 grid of TilePads to make a handheld remote control by attaching an acrylic box to the back of the pad to make it graspable. He also uses the remaining part of the sensor grid to make a wrist-worn remote control by incorporating a Velcro strap. Other forms of remote controllers such as pendant necklaces, bookmarks, paper clips, and coasters are also possible with this prototyping kit.

### Adding Interactivity to a Printed Paper with TilePads

Discrete TilePads can be used to add interactivity to a printed paper. Figure 27 illustrates a system comprising several memory tiles and a recording tile marked with the red circle. First, the user attaches three TilePads to the locations, where she


**Figure 25. (a) Self-made control panel; (b) and (c) dimming the light.**

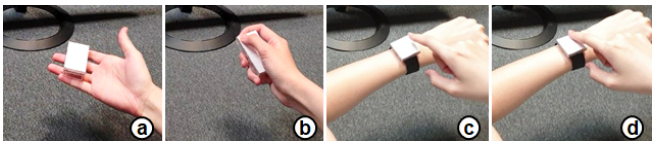


**Figure 26. (a) and (b) Handheld remote controller; (c) and (d) wrist-worn remote controller.**

wants to embed an audio message from the back of the paper. Then, she records the voice message after pressing her both hands into the recording tile and content at the same time, and releases her finger from the recording tile to finish the recording. Meanwhile, the server connected to the RFID reader updates its configuration. After that, the user can playback the audio message by touching the content. Since the binding is based on the ID at the touch location, three TilePads can record at most 27 different messages at different locations. Furthermore, the binding procedure does not require calibrations or alignments in its location or orientation since it is ID-based rather than location-based (Figure 27d). The discrete use of TilePads does not need to conform to any circuitry topology since each memory tile serves its function of sensing and data transmission.

## DISCUSSION

*Multi-touch and Contact-Shape Sensing.* Each touch-sensing point of an RFTouchPad detects touch inputs separately and sends the events to the reader independently. Hence, this infrastructure supports multi-touch inputs and the contact-shape sensing as illustrated in Figure 28a. However, when multiple tags are activated within an effective radius around the tag of a half of its free-space wave length ($\frac{\lambda}{2} \sim$16 cm), the detection becomes unstable due to the tag-to-tag interferences. Such a performance limitation makes the multi-touch and contact-shape sensing to be insufficiently supported as shown in Figure 28c. Therefore, we do not claim that the currently available sensors would support the multi-touch and contact-shape sensing, though it can be plausibly achieved by optimizing the antenna design in the future work.

*Antenna Optimization.* In this study, we aimed at optimizing the physical form of an antenna to achieve our desired functionality. We modified the conventional tags based on the design guidelines concluded based on previous research such as using the structure of the meander-line [28] and enlarging the size of the radiators to enhance the gain [20]. The form factors of the antenna are optimal for the considered applications and its performance has been improved. The change of requirements to the proposed sensor pads such as their increased size or resolution, or less-constrained thickness can be perceived as design opportunities for further performance optimization. A thorough redesign of the antenna from the engineering perspective of wireless signal optimization, such

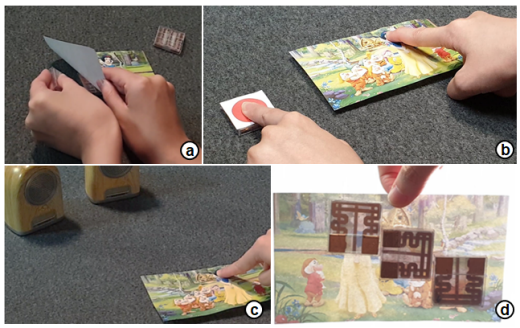

**Figure 27. Adding interactivity to a printed paper: (a) attaching TilePads to the back of the printed paper; (b) recording a message by touching both the content and recording tile button; (c) playing the message by touching the content; (d) the view from the back of the paper.**

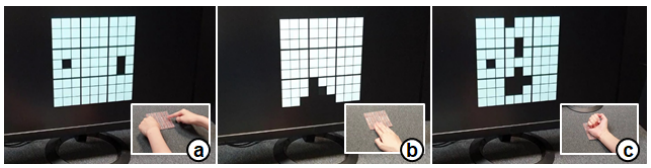

**Figure 28. (a) Multi-touch sensing; (b) contact-shape sensing; (c) a failure case.**

as optimizing the antenna impedance to minimize the body power absorption for a more compact wearable form [47], can also improve the local optimum that we achieved in our experiments presented in this paper.

*Resolution.* The pitch between the sensing points was set to 1 cm to enable the testing of each touch point individually. However, the 1-cm pitch is a bit too large for detecting fingertips, which often requires a less than 5-mm-pitch deployment [5]. Figure 29a illustrates an example of a 5-mm-pitch implementation of a StickerPad, which works the same as the original implementation (Figure 29b). The chip size should not be the main bottleneck toward a higher-resolution deployment since the Monza 4 chip used in our study for prototyping is encapsulated into a package with dimensions of 0.7 (W)$\times$0.7 (H) mm$^2$, whereas the die dimensions are only 590 (W)$\times$590 (H) $\mu$m$^2$. However, a finger touch in such a high-resolution deployment may activate multiple chips, which can impose the tag-to-tag interference problem that we discussed in the multi-touch and contact-shape sensing section. Hence, the future work should consider solutions such as a smarter algorithm and/or a more effective hardware design for increasing the sensing resolution.

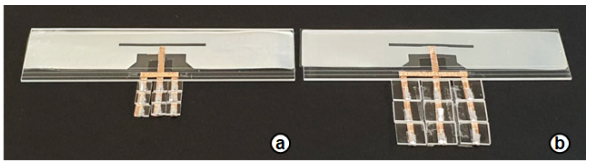

**Figure 29. (a) 5-mm-pitch StickerPad; (b) 1-cm-pitch Stickerpad.**

*Sensing Range and Deployment Cost.* The proposed system aims at supporting room-scale applications. For on-body applications, the 2-m sensing distance enabled by a single-antenna reader still depends on the tag orientation and environmental factors. Adding more antennas to the reader can effectively extend the sensing range and eliminate the blind spots in the signal coverage [11] with low outstanding hardware cost. For other applications, the StickerPads support a sensing range of 4 m, which is plausibly extensible by using a tag that supports longer-range applications (e.g., ALN-9740 tags[1]) to better accommodate rooms with different sizes. For small rooms, the deployment cost can be reduced by using cheaper UHF RFID readers (e.g., ThingMagic Nano[2]) that provide shorter sensing ranges since they support a lower power output. Applications such as prototyping and augmenting papers can still be sufficiently supported with a stationary reader installed under an unmodified non-metallic desk.

*Responsiveness.* Our current implementation suffers from the latency of the UHF tag (de)activation; hence, the consequence of a touch input is delayed for $\sim$0.5 second. Nonetheless, once the tag is read, the refresh rate of each tag read is consistently above 30 frames per second, which was tested with our 5$\times$5 grid of TilePads (Figure 20b) using the experiment apparatus illustrated in Figure 18. A previous study [11] also demonstrated that a reader (Impinj R420) can read 200 unmodified tags simultaneously at $\sim$6 fps when the tags are sufficiently separated, which implies that 200 simultaneous touch points can be handled in the same condition. The input response time can be reduced using the probabilistic filtering technique proposed by RapID [39] that can reduce the input response time to $<$ 200 ms, which would significantly improve the responsiveness and user experiences of our current implementation.

*Flexibility and Scalability of Deployment.* The two forms of the modules were designed for different purposes. The StickerPad provides flexibility, which is suitable for applications on curved surfaces such as the human body. The TilePad not only supports a more flexible deployment, supporting less-constrained placement without dealing with the potential overlapping of antennas, but also provides scalability since the tileable module is suitable for applications requiring a large sensing area. Advanced materials and manufacturing processes can enable design opportunities that are both flexible and scalable, including a TilePad with flexible substrates such as silicon or a flexible StickerPad tileable in one or more directions.

*Interference and Safety.* In addition to the aforementioned body-proximity and tag-to-tag interferences, the RFTouchPads are also sensitive to metals that can block RF signals. Therefore, the sensors should not be used in combination with metallic objects and surfaces. The deployment of RF antennas should also satisfy the specific absorption rate (SAR) limits to keep the user RF exposure below a harmful rate. The whole-body average SAR should be below 0.08 W/kg, while the SAR in the head/trunk and limbs should be lower than 2 W/kg and 4 W/kg, respectively [1, 29].

## RELATED WORK

### Sensors for 2D Touch Input

There are various types of sensors that support the sensing of touch inputs for at least 2D application. Capacitive sensors [16, 34, 5] and resistive [36, 31] touch sensor matrices are

[1]http://www.alientechnology.com
[2]https://www.jadaktech.com

the most common implementations. The sensor matrices are highly scalable [52, 36], and their form can be flexible [32, 31]. A capacitive sensor matrix can detect a finger touch on fabrics and through fabrics [38, 31], as well as be applied to human skin as patches [27] or patterns that are made of gold leaf [14]. Furthermore, there are emerging hardware touch-sensing techniques that are flexible and scalable, such as the electrical impedance tomography (EIT) [51, 52, 48] and piezoelectric sensor matrix [35]. An array of microphones can also localize a finger touch through the sound it makes [30].

While these electrical sensors provide fine-grained and less-constrained touch inputs in at least two dimensions with the requirement of scalability and flexibility sufficiently met, they should be interfaced with a signal processing unit (e.g., microcontroller) requiring to be powered, let alone the additional hardware requirements for the data transmission. Such deployment and maintenance costs limit the use of these sensors in ubiquitous computing applications.

Researchers also used cameras and computer vision to build sensing platforms for tracking touch inputs, employing a conventional RGB camera [43], an interactive surface with an embedded camera [46], an optical sensing module [9, 7, 24], or at least one depth camera [12, 8, 45, 44]. Using camera tracking touch inputs is scalable in terms of the system deployment since a camera can cover a large tracking area. Nonetheless, vision-based touch tracking suffers from line-of-sight tracking issues and therefore requires careful placement and calibration to extract the 2D touch inputs reliably. Moreover, vision-based tracking has privacy concerns [10]; hence, the location and mechanism of the tracker(s) should be disclosed to the users for ethical reasons. Such a disclosure of a sensing system may contradict to the central idea of ubiquitous computing [42].

### RFID-Based Touch Sensing

Researchers have proposed several techniques for detecting touch events as inputs by analyzing the RFID signals without modifying the employed tags. IDSense [18] recognizes the coarse-grained touch events on one tag using real-time classification of the RSSI and phase angles. RIO [33] detects one-dimensional touch movements on an RFID tag by analyzing the phase changes of signals influenced by user touches. WiSh [13] detects a touch on a shape-aware surface installed with an array of RFID tag array. RF-IDraw [41] localizes fingers by analyzing the signals of the tags worn on the fingers. 2DR [53] enables 2D touch inputs on one tag based on its custom-shape antenna and the classification of its unique phase information. These solutions require a considerable computing power for signal analysis, while their performance is affected by the environmental noise.

To increase the reliability of the touch sensing in practice, researchers have proposed to modify the tag circuitry to amplify the changes of ID-related signals as reliable signal sources. PaperID [17] enables a reliable touch sensing and widgets for constrained touch inputs through a monopole antenna design. BitID [50] presents a shorting mechanism that restarts an RFID tag based on the user touch. RFIMatch [19] detects the finger touching the tag based on the correlated state change between the tag and the tag-embedded fingerstall worn on the finger. Furthermore, there is a significant amount of work on detecting state changes of electromechanical sensors in the tag circuitry caused by human touches [40, 11, 21]. However, these solutions do not effectively extend touch inputs to 2D in a scalable way due to large antennas being employed in their circuitry.

The Wireless Identification and Sensing Platform (WISP) [37] provides custom-built RFID tags with an embedded microcontroller unit (MCU), which potentially can handle more sophisticated signals in a batteryless and wireless way [25]. Conventional solutions such as Farsens[3] battery-free RFID sensors can also interface resistive or capacitive sensors for sensing touches. However, these MCU-based solutions render constraints in their size, cost, and the user burden, making them unsuitable for the applications proposed in this paper.

Compared to previous studies, our work enables the battery-free and wireless 2D touch sensing with a multi-chip RFID tag design. Our solution does not include any batteries, wires, or microcontrollers. Furthermore, it exhibits a low computational cost and a high reliability since it uses only the presence of IDs for localizing touches, while its tileable and flexible physical design enables unconstrained 2D inputs with high scalability and flexibility.

## CONCLUSION

We presented RFTouchPads, a system of batteryless and wireless modular hardware designs of 2D touch sensor pads based on UHF RFID. We proposed two modular hardware designs, StickerPad and TilePad, and their proof-of-concept implementations. StickerPads provide flexible form factors enabling their attachment to curved surfaces easily as opposed to conventional RFID tags. TilePad supports a modular expansion of its sensing area by tiling, allowing the expanded sensing area to provide less-constrained 2D touch inputs. The proposed designs were analyzed in a series of experiments, and the results demonstrated that our current implementation can effectively support 2D touch inputs remotely from a reader. Using three applications (an on-body controller, a prototyping kit, and a paper augmentation), we demonstrated the ways of using the proposed modules, as well as their benefits. Our current results and implementations can serve as a solid basis for further investigation. The possible directions of future research for extending our current results were suggested in the discussion section. We sincerely hope that the HCI community can use this material to continue the exploration of ubiquitous computing applications.

## ACKNOWLEDGEMENTS

This research was supported in part by the Ministry of Science and Technology of Taiwan (MOST 108-2633-E-002-001), National Taiwan University (NTU-108L104039), and Intel Corporation.

## REFERENCES

[1] 2006. IEEE Standard for Safety Levels with Respect to Human Exposure to Radio Frequency Electromagnetic Fields, 3 kHz to 300 GHz. *IEEE Std C95.1-2005*

[3] http://www.farsens.com/

*(Revision of IEEE Std C95.1-1991)* (April 2006), 1–238. DOI:http://dx.doi.org/10.1109/IEEESTD.2006.99501

[2] S. Caizzone, C. Occhiuzzi, and G. Marrocco. 2011. Multi-Chip RFID Antenna Integrating Shape-Memory Alloys for Detection of Thermal Thresholds. *IEEE Transactions on Antennas and Propagation* 59, 7 (July 2011), 2488–2494. DOI: http://dx.doi.org/10.1109/TAP.2011.2152341

[3] L. Catarinucci, R. Colella, and L. Tarricone. 2009. A Cost-Effective UHF RFID Tag for Transmission of Generic Sensor Data in Wireless Sensor Networks. *IEEE Transactions on Microwave Theory and Techniques* 57, 5 (May 2009), 1291–1296. DOI: http://dx.doi.org/10.1109/TMTT.2009.2017296

[4] L. Catarinucci, R. Colella, and L. Tarricone. 2013. Enhanced UHF RFID Sensor-Tag. *IEEE Microwave and Wireless Components Letters* 23, 1 (Jan 2013), 49–51. DOI:http://dx.doi.org/10.1109/LMWC.2012.2234092

[5] Paul Dietz and Darren Leigh. 2001. DiamondTouch: A Multi-user Touch Technology. In *Proceedings of the 14th Annual ACM Symposium on User Interface Software and Technology (UIST '01)*. ACM, New York, NY, USA, 219–226. DOI: http://dx.doi.org/10.1145/502348.502389

[6] James J Gibson. The theory of affordances. (????).

[7] Jiseong Gu, Seongkook Heo, Jaehyun Han, Sunjun Kim, and Geehyuk Lee. 2013. LongPad: a touchpad using the entire area below the keyboard of a laptop computer. In *Proceedings of the SIGCHI Conference on Human Factors in Computing Systems*. ACM, 1421–1430.

[8] Chris Harrison, Hrvoje Benko, and Andrew D. Wilson. 2011. OmniTouch: Wearable Multitouch Interaction Everywhere. In *Proceedings of the 24th Annual ACM Symposium on User Interface Software and Technology (UIST '11)*. ACM, New York, NY, USA, 441–450. DOI: http://dx.doi.org/10.1145/2047196.2047255

[9] Steve Hodges, Shahram Izadi, Alex Butler, Alban Rrustemi, and Bill Buxton. 2007. ThinSight: Versatile Multi-touch Sensing for Thin Form-factor Displays. In *Proceedings of the 20th Annual ACM Symposium on User Interface Software and Technology (UIST '07)*. ACM, New York, NY, USA, 259–268. DOI: http://dx.doi.org/10.1145/1294211.1294258

[10] Jason Hong. 2013. Considering Privacy Issues in the Context of Google Glass. *Commun. ACM* 56, 11 (Nov. 2013), 10–11.

[11] Meng-Ju Hsieh, Rong-Hao Liang, Da-Yuan Huang, Jheng-You Ke, and Bing-Yu Chen. 2018. RFIBricks: Interactive Building Blocks Based on RFID. In *Proceedings of the 2018 CHI Conference on Human Factors in Computing Systems (CHI '18)*. ACM, New York, NY, USA, Article 189, 10 pages. DOI: http://dx.doi.org/10.1145/3173574.3173763

[12] Shahram Izadi, David Kim, Otmar Hilliges, David Molyneaux, Richard Newcombe, Pushmeet Kohli, Jamie Shotton, Steve Hodges, Dustin Freeman, Andrew Davison, and Andrew Fitzgibbon. 2011. KinectFusion: Real-time 3D Reconstruction and Interaction Using a Moving Depth Camera. In *Proceedings of the 24th Annual ACM Symposium on User Interface Software and Technology (UIST '11)*. ACM, New York, NY, USA, 559–568. DOI: http://dx.doi.org/10.1145/2047196.2047270

[13] Haojian Jin, Jingxian Wang, Zhijian Yang, Swarun Kumar, and Jason Hong. 2018. WiSh: Towards a Wireless Shape-aware World Using Passive RFIDs. In *Proceedings of the 16th Annual International Conference on Mobile Systems, Applications, and Services (MobiSys '18)*. ACM, New York, NY, USA, 428–441. DOI: http://dx.doi.org/10.1145/3210240.3210328

[14] Hsin-Liu (Cindy) Kao, Christian Holz, Asta Roseway, Andres Calvo, and Chris Schmandt. 2016. DuoSkin: Rapidly Prototyping On-skin User Interfaces Using Skin-friendly Materials. In *Proceedings of the 2016 ACM International Symposium on Wearable Computers (ISWC '16)*. ACM, New York, NY, USA, 16–23. DOI: http://dx.doi.org/10.1145/2971763.2971777

[15] Karoliina Koski, Elham Moradi, A Ali Babar, Toni Björninen, Lauri Sydänheimo, Leena Ukkonen, and Yahya Rahmat-Samii. 2013. Durability of embroidered antennas in wireless body-centric healthcare applications. In *2013 7th European Conference on Antennas and Propagation (EuCAP)*. IEEE, 565–569.

[16] SK Lee, William Buxton, and K. C. Smith. 1985. A Multi-touch Three Dimensional Touch-sensitive Tablet. In *Proceedings of the SIGCHI Conference on Human Factors in Computing Systems (CHI '85)*. ACM, New York, NY, USA, 21–25. DOI: http://dx.doi.org/10.1145/317456.317461

[17] Hanchuan Li, Eric Brockmeyer, Elizabeth J. Carter, Josh Fromm, Scott E. Hudson, Shwetak N. Patel, and Alanson Sample. 2016. PaperID: A Technique for Drawing Functional Battery-Free Wireless Interfaces on Paper. In *Proceedings of the 2016 CHI Conference on Human Factors in Computing Systems (CHI '16)*. ACM, New York, NY, USA, 5885–5896. DOI: http://dx.doi.org/10.1145/2858036.2858249

[18] Hanchuan Li, Can Ye, and Alanson P. Sample. 2015. IDSense: A Human Object Interaction Detection System Based on Passive UHF RFID. In *Proceedings of the 33rd Annual ACM Conference on Human Factors in Computing Systems (CHI '15)*. ACM, New York, NY, USA, 2555–2564. DOI: http://dx.doi.org/10.1145/2702123.2702178

[19] Rong-Hao Liang, Meng-Ju Hsieh, Jheng-You Ke, Jr-Ling Guo, and Bing-Yu Chen. 2018. RFIMatch: Distributed Batteryless Near-Field Identification Using RFID-Tagged Magnet-Biased Reed Switches. In *Proceedings of the 31st Annual ACM Symposium on*

*User Interface Software and Technology (UIST '18)*. ACM, New York, NY, USA, 473–483. DOI: http://dx.doi.org/10.1145/3242587.3242620

[20] Y. Lin, M. Chang, H. Chen, and B. Lai. 2016. Gain Enhancement of Ground Radiation Antenna for RFID Tag Mounted on Metallic Plane. *IEEE Transactions on Antennas and Propagation* 64, 4 (April 2016), 1193–1200. DOI: http://dx.doi.org/10.1109/TAP.2016.2526047

[21] Nicolai Marquardt, Alex S. Taylor, Nicolas Villar, and Saul Greenberg. 2010. Rethinking RFID: Awareness and Control for Interaction with RFID Systems. In *Proceedings of the SIGCHI Conference on Human Factors in Computing Systems (CHI '10)*. ACM, New York, NY, USA, 2307–2316. DOI: http://dx.doi.org/10.1145/1753326.1753674

[22] G. Marrocco. 2008. The art of UHF RFID antenna design: impedance-matching and size-reduction techniques. *IEEE Antennas and Propagation Magazine* 50, 1 (Feb 2008), 66–79. DOI: http://dx.doi.org/10.1109/MAP.2008.4494504

[23] G. Marrocco, L. Mattioni, and C. Calabrese. 2008. Multiport Sensor RFIDs for Wireless Passive Sensing of ObjectsâĂŤBasic Theory and Early Results. *IEEE Transactions on Antennas and Propagation* 56, 8 (Aug 2008), 2691–2702. DOI: http://dx.doi.org/10.1109/TAP.2008.927541

[24] Jon Moeller and Andruid Kerne. 2012. ZeroTouch: An Optical Multi-touch and Free-air Interaction Architecture. In *Proceedings of the SIGCHI Conference on Human Factors in Computing Systems (CHI '12)*. ACM, New York, NY, USA, 2165–2174. DOI: http://dx.doi.org/10.1145/2207676.2208368

[25] S. Naderiparizi, A. N. Parks, Z. Kapetanovic, B. Ransford, and J. R. Smith. 2015. WISPCam: A battery-free RFID camera. In *2015 IEEE International Conference on RFID (RFID)*. 166–173. DOI: http://dx.doi.org/10.1109/RFID.2015.7113088

[26] Paolo Nepa and Hendrik Rogier. 2015. Wearable Antennas for Off-Body Radio Links at VHF and UHF Bands: Challenges, the state of the art, and future trends below 1 GHz. *IEEE antennas and Propagation Magazine* 57, 5 (2015), 30–52.

[27] Aditya Shekhar Nittala, Anusha Withana, Narjes Pourjafarian, and Jürgen Steimle. 2018. Multi-Touch Skin: A Thin and Flexible Multi-Touch Sensor for On-Skin Input. In *Proceedings of the 2018 CHI Conference on Human Factors in Computing Systems (CHI '18)*. ACM, New York, NY, USA, Article 33, 12 pages. DOI:http://dx.doi.org/10.1145/3173574.3173607

[28] C. Occhiuzzi, C. Paggi, and G. Marrocco. 2011. Passive RFID Strain-Sensor Based on Meander-Line Antennas. *IEEE Transactions on Antennas and Propagation* 59, 12 (Dec 2011), 4836–4840. DOI: http://dx.doi.org/10.1109/TAP.2011.2165517

[29] International Commission on Non-Ionizing Radiation Protection and others. 2009. ICNIRP statement on the âĂIJguidelines for limiting exposure to time-varying electric, magnetic, and electromagnetic fields (up to 300 ghz)âĂİ. *Health physics* 97, 3 (2009), 257–258.

[30] Joseph A. Paradiso, Che King Leo, Nisha Checka, and Kaijen Hsiao. 2002. Passive Acoustic Knock Tracking for Interactive Windows. In *CHI '02 Extended Abstracts on Human Factors in Computing Systems (CHI EA '02)*. ACM, New York, NY, USA, 732–733. DOI: http://dx.doi.org/10.1145/506443.506570

[31] Patrick Parzer, Florian Perteneder, Kathrin Probst, Christian Rendl, Joanne Leong, Sarah Schuetz, Anita Vogl, Reinhard Schwoediauer, Martin Kaltenbrunner, Siegfried Bauer, and Michael Haller. 2018. RESi: A Highly Flexible, Pressure-Sensitive, Imperceptible Textile Interface Based on Resistive Yarns. In *Proceedings of the 31st Annual ACM Symposium on User Interface Software and Technology (UIST '18)*. ACM, New York, NY, USA, 745–756. DOI: http://dx.doi.org/10.1145/3242587.3242664

[32] Ivan Poupyrev, Nan-Wei Gong, Shiho Fukuhara, Mustafa Emre Karagozler, Carsten Schwesig, and Karen E. Robinson. 2016. Project Jacquard: Interactive Digital Textiles at Scale. In *Proceedings of the 2016 CHI Conference on Human Factors in Computing Systems (CHI '16)*. ACM, New York, NY, USA, 4216–4227. DOI:http://dx.doi.org/10.1145/2858036.2858176

[33] Swadhin Pradhan, Eugene Chai, Karthikeyan Sundaresan, Lili Qiu, Mohammad A. Khojastepour, and Sampath Rangarajan. 2017. RIO: A Pervasive RFID-based Touch Gesture Interface. In *Proceedings of the 23rd Annual International Conference on Mobile Computing and Networking (MobiCom '17)*. ACM, New York, NY, USA, 261–274. DOI: http://dx.doi.org/10.1145/3117811.3117818

[34] Jun Rekimoto. 2002. SmartSkin: an infrastructure for freehand manipulation on interactive surfaces. In *Proceedings of the SIGCHI conference on Human factors in computing systems*. ACM, 113–120.

[35] Christian Rendl, Patrick Greindl, Michael Haller, Martin Zirkl, Barbara Stadlober, and Paul Hartmann. 2012. PyzoFlex: Printed Piezoelectric Pressure Sensing Foil. In *Proceedings of the 25th Annual ACM Symposium on User Interface Software and Technology (UIST '12)*. ACM, New York, NY, USA, 509–518. DOI: http://dx.doi.org/10.1145/2380116.2380180

[36] Ilya Rosenberg and Ken Perlin. 2009. The UnMousePad: An Interpolating Multi-touch Force-sensing Input Pad. *ACM Trans. Graph.* 28, 3, Article 65 (July 2009), 9 pages. DOI:http://dx.doi.org/10.1145/1531326.1531371

[37] A. P. Sample, D. J. Yeager, P. S. Powledge, and J. R. Smith. 2007. Design of a Passively-Powered, Programmable Sensing Platform for UHF RFID Systems. In *2007 IEEE International Conference on RFID*. 149–156. DOI: http://dx.doi.org/10.1109/RFID.2007.346163

[38] T. Scott Saponas, Chris Harrison, and Hrvoje Benko. 2011. PocketTouch: Through-fabric Capacitive Touch Input. In *Proceedings of the 24th Annual ACM Symposium on User Interface Software and Technology (UIST '11)*. ACM, New York, NY, USA, 303–308. DOI: http://dx.doi.org/10.1145/2047196.2047235

[39] Andrew Spielberg, Alanson Sample, Scott E Hudson, Jennifer Mankoff, and James McCann. 2016. RapID: A framework for fabricating low-latency interactive objects with RFID tags. In *Proceedings of the 2016 CHI Conference on Human Factors in Computing Systems*. ACM, 5897–5908.

[40] Ju Wang, Omid Abari, and Srinivasan Keshav. 2018. Challenge: RFID Hacking for Fun and Profit. In *Proceedings of the 24th Annual International Conference on Mobile Computing and Networking (MobiCom '18)*. ACM, New York, NY, USA, 461–470. DOI:http://dx.doi.org/10.1145/3241539.3241561

[41] Jue Wang, Deepak Vasisht, and Dina Katabi. 2014. RF-IDraw: Virtual Touch Screen in the Air Using RF Signals. In *Proceedings of the 2014 ACM Conference on SIGCOMM (SIGCOMM '14)*. ACM, New York, NY, USA, 235–246. DOI: http://dx.doi.org/10.1145/2619239.2626330

[42] Mark Weiser. 1991. The Computer for the 21 st Century. *Scientific american* 265, 3 (1991), 94–105.

[43] Andrew D. Wilson. 2005. PlayAnywhere: A Compact Interactive Tabletop Projection-vision System. In *Proceedings of the 18th Annual ACM Symposium on User Interface Software and Technology (UIST '05)*. ACM, New York, NY, USA, 83–92. DOI: http://dx.doi.org/10.1145/1095034.1095047

[44] Andrew D. Wilson and Hrvoje Benko. 2010. Combining Multiple Depth Cameras and Projectors for Interactions on, Above and Between Surfaces. In *Proceedings of the 23Nd Annual ACM Symposium on User Interface Software and Technology (UIST '10)*. ACM, New York, NY, USA, 273–282. DOI: http://dx.doi.org/10.1145/1866029.1866073

[45] Robert Xiao, Chris Harrison, and Scott E. Hudson. 2013. WorldKit: Rapid and Easy Creation of Ad-hoc Interactive Applications on Everyday Surfaces. In *Proceedings of the SIGCHI Conference on Human Factors in Computing Systems (CHI '13)*. ACM, New York, NY, USA, 879–888. DOI: http://dx.doi.org/10.1145/2470654.2466113

[46] Jefferson Y. Han. 2005. Low-cost multi-touch sensing through frustrated total internal reaction. *UIST: Proceedings of the Annual ACM Symposium on User Interface Softaware and Technology* (01 2005), 115–118. DOI:http://dx.doi.org/10.1145/1095034.1095054

[47] Li Yang, Lara J Martin, Daniela Staiculescu, CP Wong, and Manos M Tentzeris. 2008. Conformal magnetic composite RFID for wearable RF and bio-monitoring applications. *IEEE transactions on microwave theory and techniques* 56, 12 (2008), 3223–3230.

[48] Sang Ho Yoon, Ke Huo, Yunbo Zhang, Guiming Chen, Luis Paredes, Subramanian Chidambaram, and Karthik Ramani. 2017. iSoft: A Customizable Soft Sensor with Real-time Continuous Contact and Stretching Sensing. In *Proceedings of the 30th Annual ACM Symposium on User Interface Software and Technology (UIST '17)*. ACM, New York, NY, USA, 665–678. DOI: http://dx.doi.org/10.1145/3126594.3126654

[49] T. Zhang, N. Becker, Y. Wang, Y. Zhou, and Y. Shi. 2017a. BitID: Easily Add Battery-Free Wireless Sensors to Everyday Objects. In *2017 IEEE International Conference on Smart Computing (SMARTCOMP)*. 1–8. DOI:http://dx.doi.org/10.1109/SMARTCOMP.2017.7946990

[50] T. Zhang, N. Becker, Y. Wang, Y. Zhou, and Y. Shi. 2017b. BitID: Easily Add Battery-Free Wireless Sensors to Everyday Objects. In *2017 IEEE International Conference on Smart Computing (SMARTCOMP)*. 1–8. DOI:http://dx.doi.org/10.1109/SMARTCOMP.2017.7946990

[51] Yang Zhang and Chris Harrison. 2018. Pulp Nonfiction: Low-Cost Touch Tracking for Paper. In *Proceedings of the 2018 CHI Conference on Human Factors in Computing Systems (CHI '18)*. ACM, New York, NY, USA, Article 117, 11 pages. DOI: http://dx.doi.org/10.1145/3173574.3173691

[52] Yang Zhang, Gierad Laput, and Chris Harrison. 2017. Electrick: Low-Cost Touch Sensing Using Electric Field Tomography. In *Proceedings of the 2017 CHI Conference on Human Factors in Computing Systems (CHI '17)*. ACM, New York, NY, USA, 1–14. DOI: http://dx.doi.org/10.1145/3025453.3025842

[53] Shilin Zhu and Yilong Li. 2018. 2DR: Towards Fine-Grained 2-D RFID Touch Sensing. *arXiv preprint arXiv:1808.08808* (2018).